

# Complex-valued interferometric inverse synthetic aperture radar image compression base on compressed sensing

Liechen Li<sup>1,2</sup>, Daojing Li<sup>1</sup>, Bo Liu<sup>3</sup>, Qingjuan Zhang<sup>4</sup>

<sup>1</sup>Science and Technology on Microwave Imaging Laboratory, Institute of Electronics, Chinese Academy of Sciences, Beijing 100190, People's Republic of China

<sup>2</sup>University of Chinese Academy of Sciences, Beijing 100049, People's Republic of China

<sup>3</sup>China Academy of Space Technology, Beijing 100094, People's Republic of China

<sup>4</sup>Patent Examination Cooperation Center Jiangsu Center of the Patent Office, SIPO, Suzhou 215011, People's Republic of China

E-mail: [chrisee365@hotmail.com](mailto:chrisee365@hotmail.com)

Published in *The Journal of Engineering*; Received on 31st January 2014; Accepted on 2nd June 2014

**Abstract:** Complex-valued interferometric inverse synthetic aperture radar (InISAR) image compression is discussed in this study. The target scene has its continuity and is compressible. However, because of the random phase of each resolution cell, the frequency spectrum of an ISAR image is wide and the complex-valued image is hard to compress. A complex-valued ISAR image compression approach is proposed. Using two or more antennas and interferometry processing, the random phase of image pixel can be cancelled and the frequency spectrum becomes sparse. Therefore the theory of compressed sensing can be introduced to the process of the complex-valued image compression. Hence, the complex-valued InISAR image compression and reconstruction can be completed. Results on real data are presented to validate the method. In comparison with results of the conventional compression techniques, the proposed method shows the better ability to preserve both the imaging magnitude and interferometric phase.

## 1 Introduction

Inverse synthetic aperture radar (ISAR) imaging is an important tool in many military and civilian applications. However, while the volume of data collected is increasing rapidly, the ability to transmit it, or to store it, is not increasing as fast. An ISAR system faces the challenge of storage and transmission of mass data. An ISAR system may collect data at a high rate that easily exceeds the capacity of the downlink channel or the volume of the mass storage medium. Moreover, the volume of data doubles or more in the ISAR interferometry case. The situation has become even more severe in the past few years with the increased requirements of modern ISAR systems, including high resolution, multi-polarisation, three-dimensional (3D) imaging, multi-frequency and multi-operation mode. As a result, effective data compression becomes necessary [1, 2].

There are mainly two approaches to compress ISAR data: compression of ISAR raw data and compression of the ISAR image acquired in real time. For ISAR raw data compression, algorithms developed can generally be divided into three categories: scalar compression algorithms, vector compression algorithms and transform domain compression algorithms [3–5]. For image compression, it is much more difficult in the ISAR case because an ISAR image differs from an optical image in several ways. The spectrum of an ISAR image tends to have less spectral rolloff than an optical image. The dynamic range of an ISAR image is typically much higher than an optical image. The ISAR image has much high-frequency energy. These make an ISAR image hard to compress. The existing methods [6–8] may compress and restore a single ISAR image well, but are hard to apply on ISAR interferometry for its high phase loss.

To make the frequency spectrum of an ISAR image narrow, interferometry technique is used. The random phases of each resolution cell are considered as the same if the two antennas are close enough. Therefore the random phase of each resolution cell can be cancelled and the spectrum of an ISAR image becomes narrow and sparse. This property suggests the using of compressed sensing (CS) [9, 10] methods for image compression and restoration. CS,

as a favourable sparse reconstruction technique, is a new and attractive method for image compression and restoration. It aims at minimising the number of measurements to be taken from signals while still retaining the information necessary to approximate them well. Compared with conventional compression techniques, CS exploits the sparsity of the signal.

The main contribution of this paper is a presentation of a new complex-valued ISAR image compression method based on CS with ISAR interferometry techniques. We proposed the idea that using the information of two antennas to shrink the range of the image frequency spectrum by introducing the interferometry techniques to cancel the random phase of each resolution cell. To compress more and restore with lower loss, we apply CS to compression processing by constructing a specially designed dictionary. Both the amplitude and phase of complex-valued ISAR images are reconstructed with overwhelming probability. Therefore, the proposed method can preserve the image phase while obtaining the magnitude at the same time. By compressing the data volume, the proposed method can release the pressure on record devices and shorten the data transmission time.

The structure of this paper is organised as follows. The next section discusses about the characters of complex-valued ISAR images and interferometry. Section 3 gives a brief introduction of CS theory. Section 4 presents the implementation the ISAR compression and restoration based on CS. In Section 5, real data experiments are made to verify the feasibility of the proposed method. Theoretical analysis and experiment results are given to assess the performance between the CS-based method and conventional low pass filter (LPF) method. Finally, the conclusions of this paper and discussion of the proposed method are provided in Section 6.

## 2 ISAR image characters

ISAR images can provide information on the surface properties of the detected targets which are always continuous in the target scene. However, the magnitude of the radar image resolution is much larger than that of wavelength, resulting in the random phase of

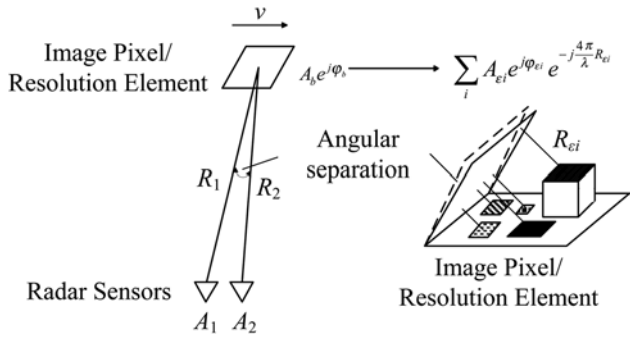


Fig. 1 Random phase mechanism

pixels which makes the scene discontinuous and spectrum wide. Fig. 1 shows the mechanism of the random phase.

As Fig. 1 depicts, pixels in radar image are a complex phasor representation of the coherent backscatter from the resolution element on the target and the propagation phase delay [11]. The propagation phase delay is determined by  $R_i$  ( $i = 1, 2$ ) which denotes the distance between radar sensors and targets. Backscatter phase delay is coherent sum of contributions from all elemental scatterers in the resolution element with backscatter and their differential path delays  $R_{ei}$ , that is

$$\varphi_b = \arg \left\{ \sum_i A_{ei} e^{j\varphi_{ei}} e^{-j(4\pi/\lambda)R_{ei}} \right\} \quad (1)$$

where  $\lambda$  is the wavelength. The total phase delay can be written as

$$\varphi = 2 \frac{2\pi}{\lambda} R + \varphi_b \quad (2)$$

The distance  $R_i$  is continuous in most cases and varies slowly, so it contributes to the low-frequency energy. Backscatter phase delay  $\varphi_b$  is random for a single ISAR image and contributes to the high-frequency energy, which makes the spectrum wide and compression hard to implement.

When the system has two antennas as is shown in Fig. 1, two images will be attained. The phase delay of each antenna can be written as

$$\begin{cases} \varphi_1 = 2 \frac{2\pi}{\lambda} R_1 + \varphi_{b1} \\ \varphi_2 = 2 \frac{2\pi}{\lambda} R_2 + \varphi_{b2} \end{cases} \quad (3)$$

If the view angle is much less than  $1^\circ$ , the coherent sum is nearly unchanged. We can suppose the random phases of two images are the same, that is,  $\varphi_{b1} = \varphi_{b2}$ . Pixels in two radar images observed from nearby vantage points have nearly the same complex phasor representation of the coherent backscatter from a resolution element on the target, but a different propagation phase delay. Although the backscatter phase delay is random for a single image, it can be cancelled using conjugate multiplication. After co-registration of two images, construct a new image similar to obtaining an interferogram as

$$s = A_2 e^{j\varphi_2} e^{-j\varphi_1} = A_2 e^{-j(4\pi/\lambda)\Delta R} \quad (4)$$

where  $\Delta R = R_1 - R_2$ . The new image removes the random phase and keeps the differential phase which can be further used. The phase delay is proportional to the range difference which is mostly

continuous in the target scene. Hence, the spectrum of the complex-valued image becomes sparse and CS theory can be introduced.

### 3 CS basis

CS is a new theory that focuses on sparse signal compression and reconstruction. For the sparse signal, CS measures  $M$  ( $K < M \ll N$ ) projections of  $\mathbf{x}$  and reconstructs the sparse signal from this small set of non-adaptive linear measurements. Each measurement can be viewed as an inner product with the signal  $\mathbf{x}$  and some vector  $\boldsymbol{\psi}_i$ . If we collect  $M$  measurements in this way, we may then consider the  $M \times N$  measurement matrix whose row are the vectors  $\boldsymbol{\psi}_i^T$ . The sparse recovery problem can be considered as the recovery of the  $K$ -sparse signal  $\mathbf{x}$  from its measurement vector  $\mathbf{y} = \boldsymbol{\Psi}\mathbf{x}$ . A direct formulation of this problem is to solve the  $\ell_0$ -minimisation problem

$$\min_{\mathbf{x} \in \mathbb{R}^N} \|\mathbf{x}\|_0, \quad \text{s.t. } \mathbf{y} = \boldsymbol{\Psi}\mathbf{x} \quad (5)$$

However,  $\ell_0$ -minimisation is computationally difficult to solve, as it involves NP-hard enumerative search. Fortunately, recent work in CS has shown that the convex relaxation approach relies on the fact that, besides the  $\ell_0$  norm, the  $\ell_1$  norm also promotes sparsity in a solution. The relaxed version of the problem can be written as

$$\min_{\mathbf{x} \in \mathbb{R}^N} \|\mathbf{x}\|_1, \quad \text{s.t. } \mathbf{y} = \boldsymbol{\Psi}\mathbf{x} \quad (6)$$

The  $\ell_1$ -minimisation approach provides uniform guarantees and stability and relies on methods in linear programming. Equation (6) requires a condition on the measurement matrix  $\boldsymbol{\Psi}$  stronger than the simple injectivity on sparse vectors, but many kinds of matrices have been shown to satisfy this condition number of measurements  $M \geq K \log N$ . Candès and Tao showed that under a slightly stronger condition, which is known as restricted isometry property (RIP), basis pursuit (BP) can recover every  $K$ -sparse signal by solving (6) [12]. The RIP requires

$$(1 - \delta)\|\mathbf{x}\|_2 \leq \|\boldsymbol{\Psi}\mathbf{x}\|_2 \leq (1 + \delta)\|\mathbf{x}\|_2 \quad (7)$$

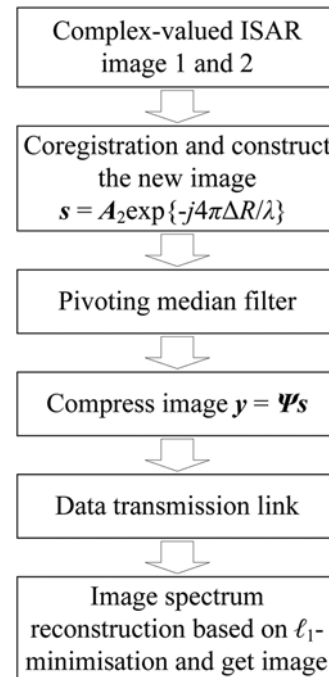
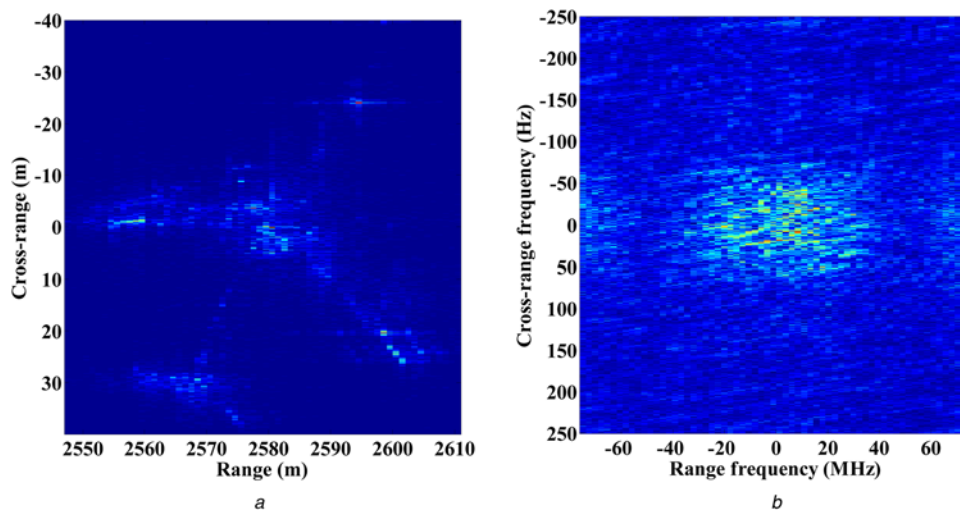


Fig. 2 Flowchart of the proposed method



**Fig. 3** Original image and frequency spectrum  
*a* The original ISAR image  
*b* The original ISAR frequency spectrum

The RIP is closely related to an incoherency property. It has been shown that with exponentially high probability, random Gaussian, Bernoulli and partial Fourier matrices satisfy the RIP with number of measurements nearly linear in the sparsity level.

When the signal  $y$  is noisy, the signal representation problem becomes a signal approximation problem. The modified convex problem can be described as

$$\min_{x \in \mathbb{R}^N} \|x\|_1, \quad \text{s.t.} \quad \|y - \Psi x\|_2 \leq \varepsilon \quad (8)$$

where  $\varepsilon$  bounds the amount of noise in measured data. Many approximate algorithms for the CS reconstruction given by (5) have also been developed, such as BP and the family of matching pursuit algorithms [13]. Note that it is known that Fourier measurements represent good projections for CS of sparse point like signals when representing random undersampling of the spatial frequency data. This suggests a natural application to the image compression problem.

#### 4 Interferometric ISAR image compression

According to the CS theory, if the image is sparse in frequency domain, sampling in time domain does not need to satisfy the

Nyquist sampling theorem. Only a few measurements are needed to reconstruct the image. As the new complex-valued ISAR image in (4) is sparse in frequency domain, it can be compressed by using the CS-based method.

The process of the complex-valued image compression can be expressed as

$$y = \Phi s + n = \Phi F \sigma + n = \Psi \sigma + n \quad (9)$$

where  $y$  is the compressed image,  $s$  is the new image to compress which takes the form as (4),  $\sigma$  is the image frequency spectrum to be reconstructed and  $n$  denotes the noise. To decrease the effect of speckle noise, pivoting median filter [14] is used on the phase of image before the compression. It is worth noting that since CS theory deals with 1D problem, 2D variables  $s$  and  $y$  must reshape into vector form.

In (9),  $\Phi$  is the projection matrix and  $F$  is a transform matrix.  $\Phi$  is designed incoherent to  $F$  and determined by the sampling sequence. For example, if the sampling sequence is [100101], where 1 stands for samplings and 0 stands for discarded samplings,  $\Phi$  can be

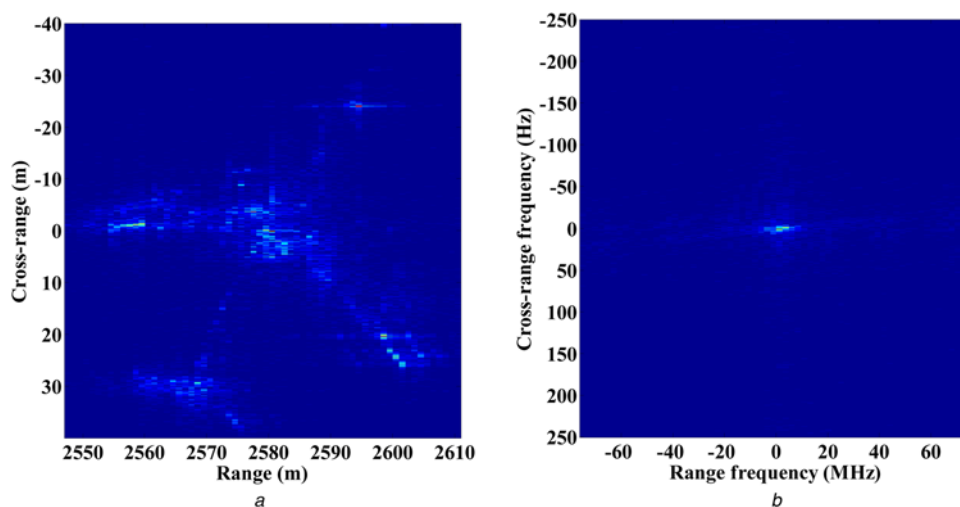


**Fig. 4** Image without random phase and frequency spectrum  
*a* The ISAR image without random phase  
*b* The frequency spectrum of the InISAR image

**Table 1** Reconstruction comparison

	MSE1	MSE2	MPE, °
CS image 1	0.0633	0.0218	35.0035
LPF image	0.0496	0.0628	25.0685
CS image 2	0.0076	0.0197	13.6379

expressed as

$$\Phi = \begin{pmatrix} 1 & 0 & 0 & 0 & 0 & 0 \\ 0 & 0 & 0 & 1 & 0 & 0 \\ 0 & 0 & 0 & 0 & 0 & 1 \end{pmatrix} \quad (10)$$

With the projection matrix  $\Phi$ , an  $N \times 1$  reshaped image  $s$  is projected on  $R^M$  space, where  $M \ll N$ , so the compression is achieved. With  $F$ , the image can be sparse represented. To reconstruct the signal with high probability, the matrix product  $\Psi = \Phi F$  has to satisfy RIP in (7). Here Fourier transform is chosen to represent

the image. Fourier basis is a simple and popular dictionary. As aforementioned, the new image  $s$  can be sparsely represented under Fourier basis. Fourier basis is also highly incoherent with the matrix  $\Phi$ , which provides a good condition for correct reconstruction.

To restore the image, the CS-based method does not reconstruct the image directly, but reconstruct the frequency spectrum of the image first and then the image [15]. The spectrum can be reconstructed by solving the optimisation problem as follows

$$\min_{\sigma \in R^V} \|\sigma\|_1, \quad \text{s.t. } \|y - \Psi\sigma\|_2 \leq \varepsilon \quad (11)$$

where  $\varepsilon$  denotes the noise level in measured data and is determined by the noise energy. After frequency spectrum of the image is reconstructed, the image can be restored simply by 2D inverse Fourier transform. After restoring the image, multiply with the phase of image 1 if needed. The main procedures are shown in Fig. 2.

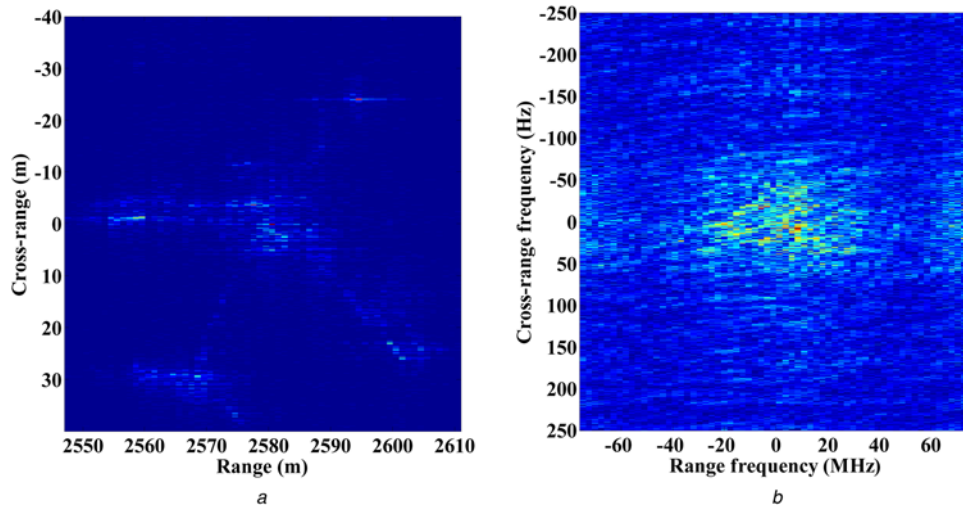


**Fig. 5** Reconstruction of the original image by CS  
*a* The reconstructed ISAR image  
*b* The reconstructed frequency spectrum

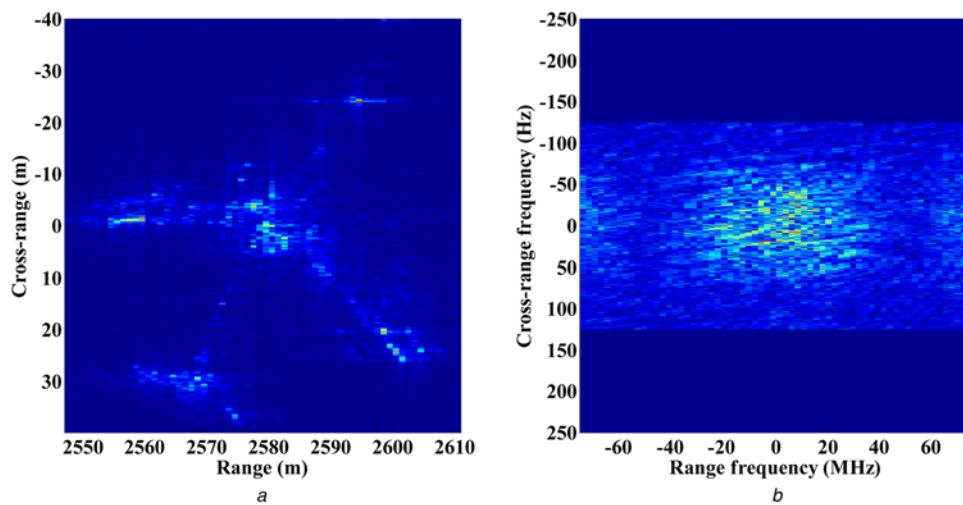


**Fig. 6** Reconstruction of the original image by LPF  
*a* The reconstructed ISAR image  
*b* The frequency spectrum after LPF

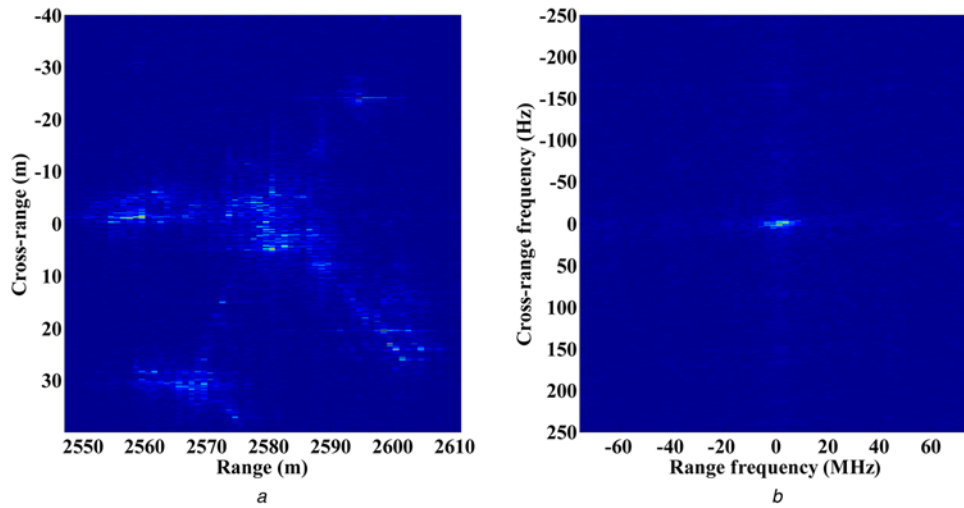


**Fig. 7** Reconstruction of the image without the random phase by CS  
*a* The reconstructed InSAR image  
*b* The reconstructed InSAR image frequency spectrum

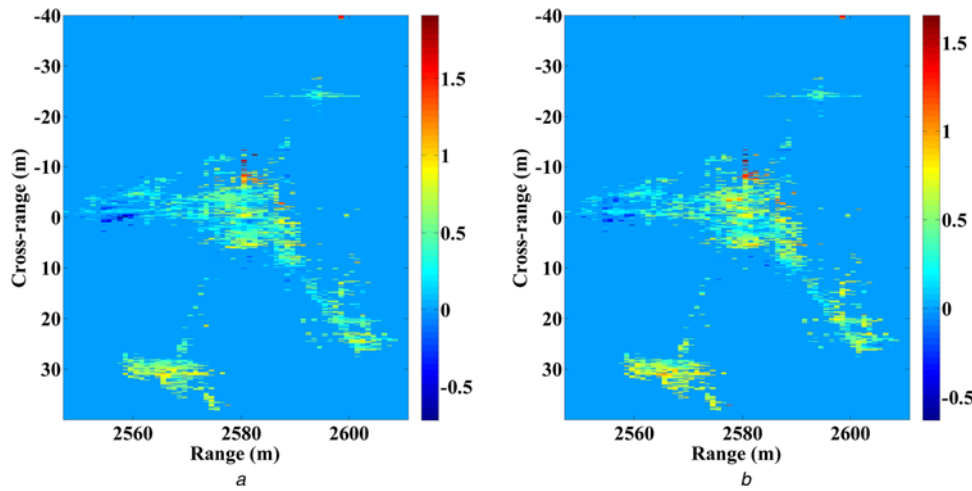


**Fig. 8** Original interferometric phase and reconstructed interferometric phase by CS  
*a* The original interferometric phase  
*b* The reconstructed interferometric phase

## 5 Real data experiments

To illustrate the feasibility of the method introduced in this paper, this section presents some results based on data obtained by a millimetre wave prototype ISAR with three antennas which is developed and operated by Institute of Electronics, Chinese Academy of Sciences. The radar works on Ka-band and the baseline between two antennas which we use is 0.4 m.

The aeroplane ISAR image shown in Fig. 3 is used as reference to compare the imaged quality of reconstructed image, where (a) is the ISAR image magnitude and (b) is the frequency spectrum of the image. The image is formed using  $\omega K$  algorithm after parameter estimation. The image constructed as (4) without random phases is shown in Fig. 4 whose frequency spectrum becomes sparse. A  $5 \times 3$  window is used in pivoting median filter. About 50% of the image is sampled to reconstruct the full frequency spectrum of the image. Gaussian random sampling and LPF are used to compress the image. To reconstruct the spectrum, BP, one of the most commonly studied  $\ell_1$ -minimisation approach, is used. Mean square error (MSE) and mean phase error (MPE) shown in (12) and (13) are used to

judge the reconstruction quality

$$\text{MSE} = \sqrt{\frac{1}{N_a N_r} \sum_{i=1}^{N_a} \sum_{j=1}^{N_r} (A_{ij} - A'_{ij})^2} \quad (12)$$

$$\text{MPE} = \frac{1}{N_a N_r} \sum_{i=1}^{N_a} \sum_{j=1}^{N_r} |P_{ij} - P'_{ij}| \quad (13)$$

where  $A$  stands for the amplitude of the image or spectrum and  $P$  denotes the phase of image. The subscripts  $i$  and  $j$  denote the  $i$ th pixel in cross-range direction and the  $j$ th pixel in range direction and the superscripts denote the reconstructed image or spectrum. Results of comparison between image to compress and reconstructed image have been listed in Table 1. MSE1 stands for the MSE of frequency spectrum and MSE2 stands for the MSE of image. CS images 1 and 2 stand for reconstruction of the original complex-valued image by CS and reconstruction of the image without the random phase by CS, respectively.

Fig. 5 shows the reconstruction of an original ISAR image by CS. Fig. 6 shows the reconstruction of the image by LPF. Both results perform poorly because of the random phases. The frequency spectrum shown in Fig. 7 is sparse which satisfies the limitation of CS. The reconstruction image quality of Fig. 7 is better than those of Figs. 5 and 6. The MSE of reconstructed image is much less than those of the other two. Image without random phases can be compressed and reconstructed with lower loss. Fig. 8a shows the original interferometric phase and Fig. 8b shows the reconstructed interferometric phase. The compression phase loss is about  $10^\circ$  and can be further used in ISAR interferometry field such as moving targets angle measurement and positioning.

## 6 Conclusions

In this paper, a CS-based approach is presented for complex-valued ISAR image compression and restoration. First the spectrum of the complex-valued ISAR image is made sparse by using the interferometric techniques. Then CS method can be introduced into compression. When the compressed image needs to be restored, it solves an optimisation problem to reconstruct the spectrum and then transform to image instead of reconstructing the image directly. Real data are used to verify the feasibility of the method proposed in this paper. The results demonstrate that the presented CS-based method can achieve better restored image quality than conventional LPF method and sparseless ISAR original images. The proposed method keeps both the amplitude and phase in the compression process. The reconstructed image can be further used in interferometry. The reconstructed complex-valued image can be further used in ISAR interferometry field. Although only the complex-valued ISAR image is investigated in this paper, the proposed concept can be also used in SAR image compression.

## 7 Acknowledgments

This work was supported by the Researching Program of Chinese Academy of Sciences and the National Natural Science Foundation of China (61271422).

## 8 References

- [1] Zeng Z., Cumming I.G.: 'SAR image data compression using a tree-structured wavelet transform', *IEEE Trans. Geosci. Remote Sens.*, 2001, **39**, (3), pp. 546–552
- [2] Hua B., Qi H.M., Zhang P., Li X.: 'Vector quantization for saturated SAR raw data compression', *Adv. Space Res.*, 2010, **45**, pp. 1330–1337
- [3] Gergič B., Planinšič P., Banjanin B., *ET AL.*: 'A comparison between SAR data compression in Cartesian and polar coordinates', *Int. J. Remote Sens.*, 2004, **25**, (10), pp. 1987–1994
- [4] Benz U., Strodl K., Moreira A.: 'A comparison of several algorithms for SAR raw data compression', *IEEE Trans. Geosci. Remote Sens.*, 1995, **33**, (5), pp. 1266–1276
- [5] Qiu X.L., Lei B., Ge Y.P., *ET AL.*: 'Performance evaluation of two compression methods for SAR raw data', *J. Electron. Inf. Technol.*, 2010, **32**, (9), pp. 2268–2272
- [6] Baxter R.A.: 'SAR image compression with the Gabor transform', *IEEE Trans. Geosci. Remote Sens.*, 1999, **37**, (1), pp. 574–588
- [7] El Assad S., Morin X., Barba D., Slavova V.: 'Compression of polarimetric synthetic aperture radar data', *Prog. Electromagn. Res.*, 2003, **39**, pp. 125–145
- [8] McGinley B., O'Halloran M., Conceicao R.C., Higgins G., Jones E., Glavin M.: 'The effects of compression on ultra wideband radar signals', *Prog. Electromagn. Res.*, 2011, **117**, pp. 51–65
- [9] Donoho D.: 'Compressed sensing', *IEEE Trans. Inf. Theory*, 2006, **52**, (4), pp. 5406–5425
- [10] Candès E., Romberg J., Tao T.: 'Robust uncertainty principles: exact signal reconstruction from highly incomplete frequency information', *IEEE Trans. Inf. Theory*, 2006, **52**, (2), pp. 489–509
- [11] Rosen P.A., Hensley S., Joughin I.R., *ET AL.*: 'Synthetic aperture radar interferometry', *Proc. IEEE*, 2000, **88**, (3), pp. 333–382
- [12] Candès E., Tao T.: 'Decoding by linear programming', *IEEE Trans. Inf. Theory*, 2005, **51**, (12), pp. 4203–4215
- [13] Needell D.: 'Topics in compressed sensing', PhD thesis, University of California, CA, USA, Davis, 2009
- [14] Meng D., Sethu V., Ambikairajah E., Ge L.: 'A novel technique for noise reduction in insar images', *IEEE Geosci. Remote Sens. Lett.*, 2007, **4**, (2), pp. 226–230
- [15] Li L., Li D., Liu B., Zhang Q., Wei L.: 'Three-aperture inverse synthetic aperture radar moving targets imaging processing based on compressive sensing'. Proc. ISICT 2012, London, UK, 2012, pp. 210–214